Vapor-Deposited Fluorinated Glycidyl Copolymer Thin Films with Low Surface Energy and Improved Mechanical Properties

Yu Mao[†] and Karen K. Gleason*[,‡]

Departments of Materials Science and Engineering and Chemical Engineering, Massachusetts Institute of Technology, Cambridge, Massachusetts 02139

Received December 4, 2005; Revised Manuscript Received February 7, 2006

ABSTRACT: Copolymer films of glycidyl methacrylate (GMA) with 2,2,3,3,4,4,5,5,6,6,7,7-dodecafluoroheptyl acrylate (DFHA) and with (perfluoroalkyl)ethyl methacrylate (PFEMA) were synthesized using initiated chemical vapor deposition (iCVD). By varying the inlet monomer feed ratios during iCVD process, the mole percentage of fluorinated acrylics in the P(GMA-*co*-DFHA) and P(GMA-*co*-PFEMA) copolymers was systematically varied between 19% and 65%. Vacuum annealing of the as-deposited copolymer films induced cross linking between epoxy functionalities of the GMA units. Both the hardness and the modulus of the annealed copolymers films were observed to increase with increasing GMA fraction, providing an order of magnitude improvement in these mechanical properties. The dispersive surface energy of the annealed copolymers showed a limited dependence on GMA fraction, with the range of values being 17.5−18.6 mN/m and 9.9−14.7 mN/m for the P(GMA-*co*-DHFA) and P(GMA-*co*-PFEMA) films, respectively. These data are as low as or lower than the benchmark value for poly(tetrafluoroethylene). The low surface energies and the limited dependence on composition suggest an enrichment of fluorinated units at the surface, a hypothesis which was directly verified using angle-resolved X-ray photoelectron spectroscopy. The annealed iCVD fluorinated copolymers also demonstrate optical transmission of greater than 99% in the visible spectrum for films with a thickness of 700 nm. The resulting combination of enhanced mechanical properties, low surface energy, and optical clarity is desirable for many applications.

Introduction

Low surface energy finishes that are also mechanically durable and optically transparent are desirable in many applications such as nonwettable, nonstick, and antifouling coatings.[1−4] Poly(tetrafluoroethylene) (PTFE, $(-CF_2-)_n$) coatings provide low surface energy with a critical surface tension (γ_c) of 18.5 mN/m[5] and a dispersive surface energy (γ_d) greater than 18 mN/m.[6,7] However, the hardness of PTFE is only 0.06 GPa,[8] while most traditional polymers exhibit hardness ∼0.2 GPa.[9] The softness of PTFE results in poor abrasion resistance. Additionally, light scattering by crystallites limits the transparency of PTFE.[10] Acrylic polymers with fluorinated side chains have even lower values of surface energy than PTFE, attributable to the comblike structure and the CF_3 end groups of their pendant chains.[11−15] Like PTFE, the mechanical properties of the fluorinated acrylate materials are poor because weak intermolecular forces between fluorinated chains limit cohesion in the coatings.[15,16] At high concentrations, the fluorinated side chains phase segregate, producing an optical haze.[15]

Copolymerization and cross linking have previously been pursued to improve the performance of fluoropolymers. Copolymerization of tetrafluoroethylene with the second component such as ethylene and perfluoromethyl vinyl ether has achieved enhanced hardness and optical clarity over PTFE.[5] Cross-linked epoxy PTFE coatings have also been reported to obtain improved hardness and modulus, with the value of 0.29 and 4.0 GPa, respectively.[17] Cross-linked hydrophobic thin films have been synthesized by pulsed plasma chemical vapor deposition (CVD) of 1*H*,1*H*,2*H*,2*H*-heptadecafluorodecyl acrylate.[18] The pulsing minimizes, but does not eliminate, loss of the fluorinated pendant group from the monomer by the plasma excitation. Additionally, knowledge of the exact chemical nature and systematic control over cross link density are difficult to obtain in pulsed plasma deposited films. Typical growth rates for pulsed plasma deposition of fluorinated monomers are in the range 5−50 nm/min.[18,19]

Systematic control over composition is essential for fundamental understanding of the multiple factors inducing the tradeoffs between mechanical properties, surface energy, and optical transparency. This work describes the synthesis and property evaluation of two series of copolymers of systematically varied bulk composition. For the first series, 2,2,3,3,4,4,5,5,6,6,7,7-dodecafluoroheptyl acrylate (DFHA, $CH_2{=}CHCOOCH_2(CF_2)_5CF_2H$) is copolymerized with glycidyl methacrylate (GMA) to create P(GMA-*co*-DFHA) films with varying degrees of GMA incorporation. The second series is similar with the exception that 2-(perfluoroalkyl)ethyl methacrylate (PFEMA, $CH_2{=}C(CH_3)COOCH_2CH_2(CF_2)_nCF_3$, $n = 5-13$, $n_{average} = 8$) is used as the monomer, resulting in P(GMA-*co*-PFEMA) films. Post-deposition heating of both series of GMA containing films was used to induce the ring opening of epoxy groups[20,21] and thus initialize the self-cross linking reactions between pairs of epoxy groups, resulting in cross links with a well-defined chemical structure and known maximum density. No initiators or catalysts were used in the cross linking reaction. Films were synthesized by initiated chemical vapor deposition (iCVD).

Background: Initiated Chemical Vapor Deposition (iCVD)

The iCVD method is a one-step synthesis technique, involving the thermal decomposition of an initiator over heated filaments and subsequent free radical polymerization of the monomer to form a film on a cooled substrate.[22−25] No plasma excitation is required. With *tert*-butyl peroxide (TBP) as the initiator, iCVD

* To whom correspondence should be addressed: e-mail kkgleasn@mit.edu; Ph (617) 253-5066.
[†] Department of Materials Science and Engineering.
[‡] Department of Chemical Engineering.

10.1021/ma052591p CCC: $33.50
Published on Web 04/27/2006

Table 1. Details of DFHA and PFEMA Copolymer Deposition

sample	filament temp (°C)	pressure (mTorr)	flow rate (sccm) fluorinated monomer	flow rate (sccm) GMA	flow rate (sccm) TBP	deposition time (min)	thickness (μm)
"D"series							
D0	220	0.3	0.80		0.10	10.2	1.22
D27	230	0.5	0.10	0.80	0.10	9.7	1.46
D45	230	0.5	0.22	0.80	0.10	9.0	1.35
D65	230	0.5	0.65	0.80	0.10	8.5	1.28
"P"series							
P0	250	0.2	0.70		0.10	8.4	1.52
P19	250	0.3	0.08	0.80	0.10	8.5	1.37
P48	250	0.3	0.24	0.80	0.10	7.8	1.25
P65	250	0.3	0.72	0.80	0.10	8.2	1.32

has successfully deposited poly(glycidyl methacrylate) (PGMA) thin films with full retention of the pendant epoxy groups[22] and poly(2-(perfluoroalkyl)ethyl methacrylate) (PPFEMA) homopolymer films with fully intact perfluoroalkyl chains.[23] The weak peroxide bond in TBP allows use of very low filament temperatures (180−250 °C) to generate radicals, which limits undesirable reactions such as further fragmentation of TBP into methyl radicals[26,27] and the destruction of the fragile pendant groups. Despite the low power input into the reactor (<5 W/cm^2), deposition rates of >150 nm/min can be achieved by iCVD.[22]

iCVD copolymerization provides the capability to further tune film composition. The process involves an initiation step in the heated vapor phase to form primary radicals followed by the adding of two different monomers to the propagating chain radical on the substrate surface, as suggested by the study of monomer reactivity ratios and copolymer molecular weights.[28] Copolymer composition can be systematically controlled by varying the gas feed ratio of two monomers into the iCVD reactor.[28,29]

The iCVD method shares many advantages in common with other chemical vapor deposition (CVD) methods. The positive features include uniform coverage over large areas, low surface roughness, and conformal coatings.[30] Because it is a dry process, CVD thin films can be grown on soluble substrates and thus can be extended to a wide range of new material applications. In addition, CVD provides the capability to coat nanoscale features[31] as well as substrates with complex geometries. From the perspective of thin film processing, CVD serves as a promising method to avoid the harsh conditions in the traditional synthesis of low surface energy coatings, since PTFE and fluorinated acrylic polymers generally require sintering conditions or special solvents to create the final coatings.[14,15] For iCVD, although the filaments are heated, the deposition surface is cooled, typically to 25−35 °C, allowing coating of thermally sensitive substrates.

Experimental Section

Films were deposited onto 100 mm diameter silicon wafer or 75 mm × 25 mm glass slide substrates in a custom-built reactor.[32] The reactor was equipped with a stainless steel filament array, which was resistively heated to 220−250 °C to thermally decompose the initiator, and a water-cooled stage (35 °C) on which the substrate was placed. The initiator half-lives at 220, 230, and 250 °C are 8.1, 4.0, and 1.0 s, respectively.[33] Pressure in the vacuum chamber was maintained using a throttling butterfly valve. GMA (97%, Aldrich), DFHA (95%, Aldrich), and PFEMA (Aldrich) were vaporized in glass jars that were heated to 62, 75, and 90 °C, respectively. TBP (98%, Aldrich) was used as the initiator and vaporized at room temperature. All vapors were mixed together before entering the reactor through a side port.

For both series of the DFHA copolymer and the PFEMA copolymer, the flow rates of TBP and GMA were regulated using needle valves and kept constant at 0.1 and 0.8 sccm, while the flow rates of DFHA and PFEMA were varied to synthesize copolymers of different compositions. Details of the experimental runs are listed in Table 1. The P(GMA-*co*-DFHA) series are labeled as "D" followed by the mole percentage of DFHA units in the film. The analysis of the DFHA percentage is discussed in the Results and Discussion section. Similarly, the labels for the P(GMA-*co*-PFEMA) series begin with "P" followed by PFEMA content in percent. D0 and P0 represent the homopolymers of DFHA and PFEMA, respectively.

After the deposition, samples were annealed in a vacuum oven with a temperature of 200 °C. The annealing temperature was chosen to avoid thermal decomposition of ester side groups in acrylic copolymers.[34] The final film thickness on silicon wafers was 1.2−1.5 μm, measured using variable-angle spectroscopic ellipsometry (VASE) with the Cauchy−Urbach model used for data fitting. The thickness of films on glass substrates was ∼710 nm as measured by profilometry (Tencor P10).

Fourier transform infrared (FTIR) measurements were done on a Nicolet Nexus 870 spectrometer in normal transmission mode using a DTGS KBr detector over the range of 400−4000 cm^{-1} at 4 cm^{-1} resolution. Angle-resolved X-ray photoelectron spectroscopy (ARXPS) was performed on a Kratos Axis Ultra spectrometer using a monochromatized aluminum Kα source at take-off angles of 20°, 55°, and 90°. Contact angle measurements were performed on five points in ∼3 cm^2 using a goniometer equipped with an automatic dispenser (Ramé-Hart). Water and a series of anhydrous linear alkanes (hexane, heptane, octane, decane, dodecane, and hexadecane, purity ≥99%) were used as test liquids. Optical transparency measurement was done on films deposited on glass substrates. The transmission of thin films was measured by a FluoroMax-2 UV−vis spectrometer within the wavelength range of 400−800 nm using air as a reference.

Measurements of hardness and elastic modulus were performed using a Nano Indenter XP (Nano Instruments) and MTS continuous stiffness measurement technique. A Berkovick diamond tip was used in the measurements. Film thicknesses of >1 μm were used to minimize any substrate effects. Measurements at 10 points were taken for each sample. It is generally accepted that the substrate impact is minimal at penetration depths of less than 10% of the film thickness.[35,36] Therefore, following standard protocol, the hardness is reported at 10% of the film thickness and the modulus is taken at 50 nm. Film surface roughness was measured using atomic force microscopy performed on a Digital Instruments Dimension 3000 under tapping mode.

Results and Discussion

Figure 1 shows the FTIR spectra of PGMA homopolymer, PDFHA homopolymer (D0), and the P(GMA-*co*-DFHA) copolymer (D45) as-deposited and after annealing (D45′). The strong absorption ranging from 1150 to 1220 cm^{-1} in D0 is assigned to CF_2 stretching,[37] and the small peak at 909 cm^{-1} in PGMA is the characteristic absorption peak of the epoxy group.[38] The spectrum of copolymer D45 displays the characteristic epoxy absorption and the CF_2 stretching, indicating

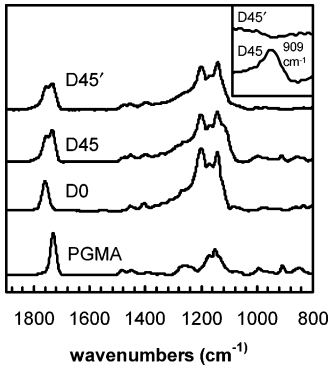

Figure 1. FTIR spectra of homopolymer PGMA, homopolymer PDFHA (D0), and copolymer as-deposited (D45) and after annealing 14 h (D45′).

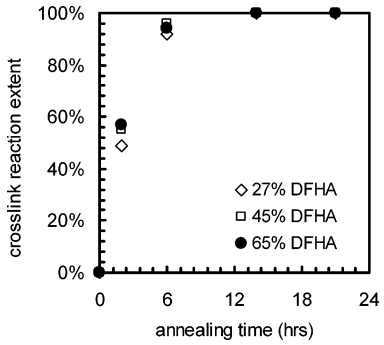

Figure 2. Cross-linking extent of epoxy groups in P(GMA-*co*-DFHA) copolymers (series "D") calculated from the absorption intensity change in the FTIR epoxy peak at 909 cm^{-1}.

incorporation of both GMA and DFHA components. In the spectrum of D45′, the 909 cm^{-1} absorption peak disappears, providing evidence for the epoxy ring-opening reaction to form cross links.

The DFHA copolymer compositions were analyzed on the basis of the Beer−Lambert equation[39] under the assumption that the C═O bond oscillator coefficient is the same in the GMA and DFHA components, as verified in other acrylic copolymers.[25] The DFHA mole fraction in the film was calculated using the equation $f_{DFHA} = 1 - A_{epoxy}/rA_{C=O}$, where r is the peak area ratio of epoxy and C═O absorption in homopolymer PGMA, A_{epoxy} is the peak area of epoxy at 909 cm^{-1}, and $A_{C=O}$ is the peak area for C═O absorption from both GMA (1730 cm^{-1}) and DFHA (1760 cm^{-1}). The results were used to label the samples in Table 1. Similarly, the extent of reaction, X, for the conversion of epoxy groups into cross links in the annealed copolymer samples can be calculated from the epoxy absorption peak area after annealing (A'_{epoxy}) and before annealing (A_{epoxy}): $X = 1 - A'_{epoxy}/A_{epoxy}$. As shown in Figure 2, P(GMA-*co*-DFHA) copolymers with different compositions demonstrate similar cross linking reaction trends with time. More than 90% of epoxy groups have reacted after vacuum annealing for 6 h at 200 °C, and complete cross link reaction of epoxy groups was achieved in 14 h.

Figure 3 shows the mechanical property changes of P(GMA-*co*-DFHA) copolymer thin films after annealing. Both the hardness and modulus of the films improve significantly. For example, the hardness of D27 increases from 0.06 to 0.36 GPa after annealing 6 h, and its modulus increases from 1.3 to 5.8 GPa. The slower rate of improvement in mechanical properties after annealing 6 h is probably due to the near completion of epoxy cross linking reaction, as indicated in Figure 2. The slight decrease of hardness and modulus after 21 h of annealing is

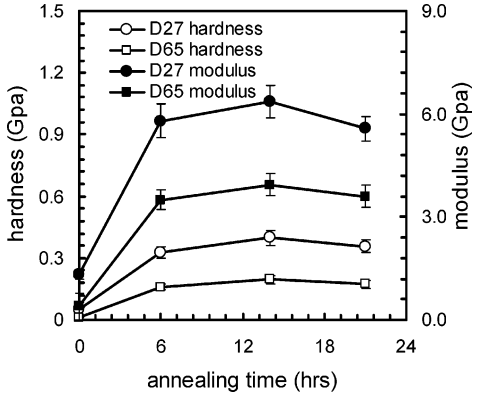

Figure 3. Mechanical property improvement of annealed P(GMA-*co*-DFHA) copolymers with 27% and 65% DFHA.

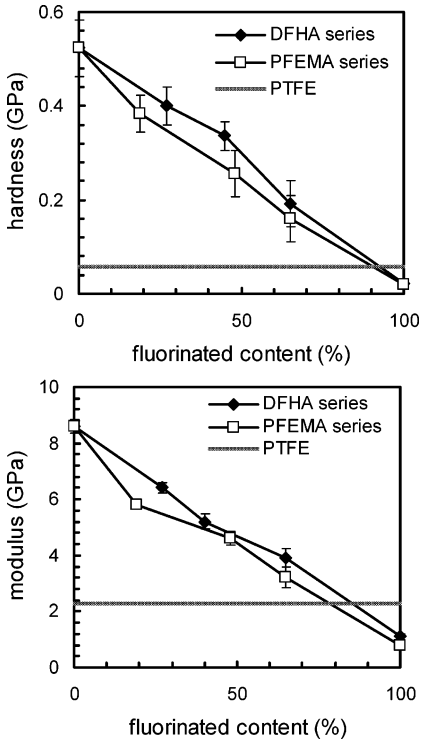

Figure 4. Mechanical properties of P(GMA-*co*-DFHA) and P(GMA-*co*-PFEMA) seriespolymers after annealing 14 h. Both PFEMA and DFHA copolymers demonstrate enhancement in hardness and modulus compared with PTFE.[8,41]

attributed to the onset of film decomposition, which can be inferred from the broadening of the C═O absorption peak in the FTIR spectra (not shown).

P(GMA-*co*-PFEMA) copolymer thin films with different PFEMA compositions were also synthesized using iCVD and analyzed using the FTIR method as discussed for the P(GMA-*co*-DFHA) copolymers. Figure 4 summarizes the hardness and modulus of both P(GMA-*co*-DFHA) and P(GMA-*co*-PFEMA) copolymers after annealing 14 h, compared with the mechanical properties of PDFHA, PPFEMA, and PTFE. The hardness of annealed DFHA and PFEMA copolymers improves 10 times compared with the hardness of DFHA and PFEMA homopolymers, and their moduli increase more than 7 times. Both the hardness and the modulus decrease as the fraction of fluorinated monomer increase because of the increasing amount of weak intermolecular cohesion between fluorinated chains. With an equal amount of fluorine-containing monomer, P(GMA-*co*-PFEMA) shows slightly lower values of modulus and hardness than P(GMA-*co*-DFHA), indicating smaller cohesion forces

Table 2. Contact Angles of Three Different Solvents on P(GMA-*co*-DFHA) and P(GMA-*co*-PFEMA) Copolymer Thin Films after Annealing for 14 h

solvent	advancing angle (deg)	receding angle (deg)	stationary angle (deg)
	27% DFHA		
octane	29.0 ± 0.4	27.6 ± 0.4	28.5 ± 0.7
hexadecane	49.6 ± 0.5	48.0 ± 0.6	49.1 ± 0.6
water	97.7 ± 0.5	76.6 ± 0.5	91.8 ± 0.5
	45% DFHA		
octane	31.0 ± 0.4	28.6 ± 0.5	30.2 ± 0.5
hexadecane	50.9 ± 0.4	49.2 ± 0.4	50.6 ± 0.2
water	99.6 ± 0.3	77.1 ± 0.4	95.4 ± 0.4
	65% DFHA		
octane	35.2 ± 0.4	33.8 ± 0.3	34.7 ± 0.5
hexadecane	52.8 ± 0.2	51.2 ± 0.2	52.3 ± 0.3
water	102.2 ± 0.3	78.9 ± 0.4	98.6 ± 0.3
	19% PFEMA		
octane	47.9 ± 0.6	46.0 ± 0.5	47.5 ± 0.4
hexadecane	62.5 ± 0.7	60.1 ± 0.6	62.1 ± 0.5
water	120.2 ± 0.5	78.9 ± 0.7	98.6 ± 0.5
	48% PFEMA		
octane	60.2 ± 0.4	58.0 ± 0.5	59.5 ± 0.4
hexadecane	73.7 ± 0.3	72.0 ± 0.3	73.5 ± 0.5
water	123.6 ± 0.4	88.7 ± 0.3	115.3 ± 0.2
	65% PFEMA		
octane	65.0 ± 0.3	63.1 ± 0.4	64.8 ± 0.2
hexadecane	79.6 ± 0.2	77.4 ± 0.3	79.0 ± 0.3
water	126.9 ± 0.2	90.3 ± 0.3	118.8 ± 0.3

between perfluorinated chains compared with the $-(CF_2)_n-CF_2H$ chains.

Table 2 lists contact angles of three different solvents on P(GMA-*co*-DFHA) and P(GMA-*co*-PFEMA) copolymer thin films annealed for 14 h. Compared to P(GMA-*co*-DFHA) with CF_2H-terminated side chains, P(GMA-*co*-PFEMA) with CF_3-terminated side chains demonstrates much higher hydrophobicity. Indeed, the advancing contact angle (θ_{ad}) is greater than 120° for water for all three PFEMA copolymer films. The high values of contact angles resulting with small amount of PFEMA incorporation suggest segregation of low-surface-energy fluorinated segments to the air−polymer interface.[16] With increasing fluorine content, the contact angle of water and other dispersive liquids on P(GMA-*co*-PFEMA) increases, indicating decrease in wettability and surface energy. It is noteworthy that these thin films exhibit extremely small root-mean-square roughness, 0.3−0.8 nm. The smoothness of these films precludes the cause of hydrophobicity due to surface roughness.[3,40] Therefore, the data represent the intrinsic wettability that is associated with the molecular structure of the thin films.

Measurement of surface energy is not straightforward, and methods based on contact angle are usually used for practical reasons.[16,18,41] The Zisman plot was widely applied to determine the critical surface tension of a surface (γ_c).[42] It must be noted that there is no theoretical justification for equating γ_c with the surface energy of a material. An alternative is to calculate the dispersion force component of the surface energy (γ_d), using the Girifalco−Good−Fowkes−Young equation.[41,43,44] For purpose of systematic comparison, Table 3 summarizes the Zisman critical surface tension and dispersive surface energy for P(GMA-*co*-DFHA) and P(GMA-*co*-PFEMA) copolymers annealed for 6 and 14 h. PFEMA copolymers, with CF_3 pendant end groups, demonstrate much lower surface energies than DFHA copolymers, with CF_2H pendant end groups. The surface energies of copolymers were observed to improve as annealing time increase from 6 to 14 h. This improvement can be attributed to a higher degree of immobilization of fluoroalkyl groups after a longer annealing time.[45]

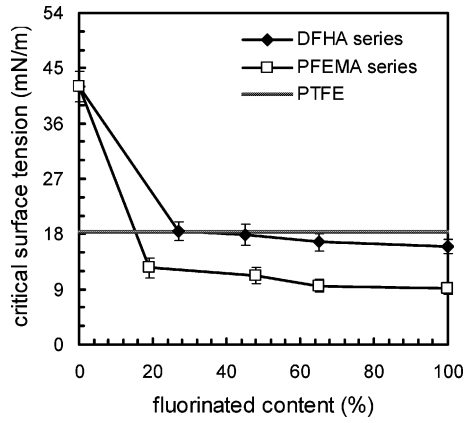

Figure 5. Critical surface tension (γ_c) of annealed P(GMA-*co*-DFHA) and P(GMA-*co*-PFEMA) series polymers, compared with the γ_c of PTFE.[5]

Table 3. Zisman Critical Surface Tension (γ_c) and Dispersive Surface Energy (γ_d) of Postannealed P(GMA-*co*-DFHA) and P(GMA-*co*-PFEMA) Copolymer Thin Films

	annealed 6 h		annealed 14 h	
sample	γ_c (mN/m)	γ_d (mN/m)	γ_c (mN/m)	γ_d (mN/m)
D27	19.2 ± 2.5	20.3 ± 0.5	18.4 ± 1.5	18.6 ± 0.4
D45	18.9 ± 2.4	19.5 ± 0.6	17.8 ± 1.7	18.2 ±0.4
D65	17.9 ± 1.8	18.1 ± 0.3	16.7 ± 1.4	17.5 ± 0.4
P19	13.3 ± 1.4	15.2 ± 0.5	12.5 ± 1.4	14.7 ± 0.3
P48	12.4 ± 1.7	12.6 ± 0.3	11.2 ± 1.6	11.8 ± 0.3
P65	10.8 ± 1.2	11.6 ± 0.3	9.6 ± 1.0	9.9 ± 0.2

Table 4. Fluorine Surface Segregation Data of P(GMA-*co*-PFEMA) Copolymer Thin Films after Annealing 14 h

PFEMA content (%)	F/C atomic ratio		XPS sampling depth (nm)
	bulk	XPS	
48	0.84	1.40	2.7
		1.24	6.6
		1.20	8.0
65	1.01	1.54	2.7
		1.37	6.6
		1.35	8.0

Figure 5 compares the critical surface tension of the DFHA and PFEMA series polymers after annealing 14 h with that of PTFE and annealed PGMA. All the annealed copolymers demonstrate lower critical surface tension than the benchmark PTFE. In both DFHA and PFEMA copolymers, the critical surface tension is observed to drop sharply with only small amount addition of fluorinated monomer. The critical surface tension of DFHA and PFEMA copolymers shows little variation with the fraction of fluorinated monomer. With the same amount of fluorinated monomer, the critical surface tension of PFEMA copolymers is much smaller than that of the DFHA copolymers, which is attributed to the difference between CF_3 and CF_2H chemistry.

ARXPS was used to quantify the fluorine to carbon (F/C) atomic ratios as a function of sampling depth in P(GMA-*co*-PFEMA) copolymers after 14 h annealing. Sampling depths (depth = $3\lambda \sin\theta$) were calculated on the basis of the take-off angle (θ) and the photoelectron escape depth (λ) estimated by Schmidt et al.[2] The results are shown in Table 4. The bulk F/C atomic ratios were calculated from the mole fractions of fluorinated acrylics obtained from the FTIR composition analysis. The F/C ratios in the first 8 nm of the surface are much higher than the bulk F/C ratios. As the sampling depth increases, the F/C ratio decreases, indicating that the lower-surface-energy perfluorinated segment segregates to the air−polymer interface. No minimum F/C ratios were observed in

the first 8 nm of the surface. Often when surfaces become enriched in fluorine, there is a fluorine-depleted subsurface region.[2] However, this is not always observed, and a continuous drop of fluorine concentration below the surface was seen in fluorinated copolymer coatings prepared from solution polymerization and spin-casting.[16,46] The iCVD polymers show a similar lack of fluorine-depleted region. The surface enrichment of fluorine content explains the low surface energies of annealed P48 ($\gamma_d = 11.8$ mN/m) and P65 ($\gamma_d = 9.9$ mN/m). The high observed F/C ratios at the surface (>1.2) and the low values of surface energies suggest rather closely packed perfluorinated segments at the surface, which has been observed previously in solution synthesized methacrylate polymers.[16]

The vapor-deposited DFHA and PFEMA copolymer thin films exhibit excellent transparency within the visible wavelength range. The transmission of all the annealed P(GMA-*co*-DFHA) copolymer thin films (thickness 712 ± 18 nm) is greater than 99.9% over the wavelength region 400−800 nm. The transmission of PFEMA copolymer thin films (thickness 715 ± 25 nm) is slightly lower than the DFHA copolymers because perfluorinated chains are more likely to form separate domains from the hydrocarbon portion of the polymer, resulting in slight haze in the final thin films. Nevertheless, the annealed PFEMA copolymers exhibit more than 99% transmission across the entire visible spectrum. These results are higher than the value reported for transparent superhydrophobic thin films.[4] The improvement of optical transparency can be attributed to (1) the GMA component copolymerized into the films and (2) the cross linking structure formed after annealing. These two changes in film structure contribute to a decrease in the crystalline component[10] and thus an enhancement in the optical transmission.

Conclusions

Fluorinated copolymer thin films with combination of enhanced mechanical properties, low surface energy, and optical clarity were synthesized. The synthesis involves iCVD copolymerization of fluorinated acrylics with GMA followed by vacuum annealing that converts glycidyl component into crosslinks. The iCVD method allowed systematic variation of the GMA fraction incorporated into the copolymers, which is critical to the bulk mechanical properties of annealed copolymer thin films. Both modulus and hardness were significantly improved as higher fractions of GMA units were incorporated into the copolymers. At GMA fraction greater than 55%, DFHA and PFEMA copolymer films exhibit more than 10-fold and 7-fold improvement in hardness and modulus over their fluorinated homopolymers, respectively. The achieved hardness and modulus in the cross linked fluorinated thin films are significantly higher than the values reported for wear-resistant fluorinated coatings.

All of the annealed copolymers were found to exhibit low surface energy and good optical transparency at all GMA fractions synthesized. The segregation of fluorine to the film surface contributes to the retention of the desired low surface energy even at low fluorine contents in the copolymer films. The surface energies of the P(GMA-*co*-PFEMA) were consistently lower than their P(GMA-*co*-DFHA) counterparts at equivalent percentages of GMA incorporation.

The optimal performance among the films synthesized in this study was post-annealed P(GMA-*co*-PFEMA) with 19% PFEMA, which simultaneously provided low surface energy ($\gamma_d = 14.7$ mN/m), high hardness (0.38 GPa) and modulus (5.8 GPa), and high transmission of visible light (99.3%). Increasing the GMA fraction may further enhance the mechanical properties without significant degradation of the surface and optical qualities. A graded coating with a high or even 100% GMA content throughout most of its thickness, transitioning to a thin surface region of high PFEMA concentration, may provide substantial improvement. Films with such graded composition are possible to envision by the iCVD synthesis method where the gas feed ratio of the GMA and PFEMA monomers are varied during the course of the deposition.

Acknowledgment. We gratefully acknowledge the support of the NSF/SRC Engineering Research Center for Environmentally Benign Semiconductor Manufacturing. This work made use of MRSEC Shared Facilities supported by the National Science Foundation under Award DMR-9400334. We also thank Dr. Qingguo Wu for help in nanoindentation experiments.

References and Notes

(1) Lindner, E. *Biofouling* **1992**, *6*, 193.
(2) Schmidt, D. L.; Coburn, C. E.; Dekoven, B. M.; Potter, G. E.; Meyers, G. F.; Fischer, D. A. *Nature* **1994**, *368*, 39.
(3) Hozumi, A.; Takai, O. *Thin Solid Films* **1997**, *303*, 222.
(4) Nakajima, A. *J. Ceram. Soc. Jpn.* **2004**, *112*, 533.
(5) Ellis, B. *Polymers—A Property Database*, CD-ROM ed.; CRC: Boca Raton, FL, 2000.
(6) Tian, J.; Xue, Q. *J. Appl. Polym. Sci.*. **1998**, *69*, 435.
(7) Rathod, N.; Hatzikiriakos, S. G. *Polym. Eng. Sci.* **2004**, *44*, 1543.
(8) Wang, J.; Shi, F. G.; Nieh, T. G.; Zhao, B.; Brongo, M. R.; Qu, S.; Rosenmayer, T. *Scr. Mater.* **2000**, *42*, 687.
(9) Briscoe, B. J.; Fiori, L.; Pelillo, E. *J. Phys. D: Appl. Phys.* **1998**, *31*, 2395.
(10) Oshima, A.; Ikeda, S.; Katoh, E.; Tabata, Y. *Radiat. Phys. Chem.* **2001**, *62*, 39.
(11) Wu, S. H. *Polymer Interfaces and Adhesion*; Marcel Dekker: New York, 1982.
(12) Zisman, W. A. In *Advances in Chemistry Series 43*; Gould, R. F., Ed. American Chemical Society: Washington, DC, 1964.
(13) Wang, J. G.; Mao, G. P.; Ober, C. K.; Krammer, E. J. *Macromolecules* **1997**, *30*, 1906.
(14) Tsibouklis, J.; Nevell, T. G. *Adv. Mater.* **2003**, *15*, 647.
(15) Anton, D. *Adv. Mater.* **1998**, *10*, 1197.
(16) Thomas, R. R.; Anton, D. R.; Graham, W. F.; Darmon, M. J.; Sauer, B. B.; Stika, K. M.; Swartzfager, D. G. *Macromolecules* **1997**, *30*, 2883.
(17) McCook, N. L.; Burris, D. L.; Bourne, G. R.; Steffens, J.; Hanrahan, J. R.; Sawyer, W. G. *Tribol. Lett.* **2005**, *18*, 119.
(18) Coulson, S. R.; Woodward, I. S.; Badyal, J. P. S.; Brewer, S. A.; Willis, C. *Chem. Mater.* **2000**, *12*, 2031.
(19) Hynes, A.; Badyal, J. P. S. *Chem. Mater.* **1998**, *10*, 2177.
(20) Smaoui, H.; Guermazi, H.; Agnel, S.; Mlik, Y.; Toureille, A.; Schue, F. *Polym. Int.* **2003**, *52*, 1287.
(21) Thompson, L. F.; Willson, C. G. *Introduction to Microlithography*, 2nd ed.; American Chemical Society: Washington, DC, 1994.
(22) Mao, Y.; Gleason, K. K. *Langmuir* **2004**, *20*, 2484.
(23) Ma, M.; Mao, Y.; Gupta, M.; Gleason, K. K.; Rutledge, G. *Macromolecules* **2005**, *38*, 9742.
(24) Chan, K.; Gleason, K. K. *Langmuir* **2005**, *21*, 11773.
(25) Chan, K.; Gleason, K. K. *Langmuir* **2005**, *21*, 8930.
(26) Goos, E.; Hippler, H.; Hoyermann, K.; Jurges, B. *Phys. Chem. Chem. Phys.* **2000**, *2*, 5127.
(27) Weber, M.; Fischer, H. *J. Am. Chem. Soc.* **1999**, *121*, 7381.
(28) Mao, Y.; Gleason, K. K. *Langmuir* **2006**, *22*, 1795.
(29) Chan, K.; Gleason, K. K. *Chem. Vap. Deposition* **2005**, *11*, 437.
(30) Pierson, H. O. *Handbook of Chemical Vapor Deposition*, 2nd ed.; Noyes Publications: Norwich, NY, 1999.
(31) Lau, K. K. S.; Bico, J.; Teo, K. B. K.; Chhowalla, M.; Amaratunga, G. A. J.; Milne, W. I.; McKinley, G. H.; Gleason, K. K. *Nano Lett.* **2003**, *3*, 1701.
(32) Mao, Y.; Felix, N. M.; Nguyen, P. T.; Ober, C. K.; Gleason, K. K. *J. Vac. Sci. Technol. B* **2004**, *22*, 2473.
(33) Odian, G. *Principles of Polymerization*, 2nd ed.; Wiley-Interscience: New York, 1981.
(34) Ito, H.; Ueda, M. *Macromolecules* **1988**, *21*, 1475.
(35) Oliver, W. C.; Pharr, G. M. *J. Mater. Res.* **1992**, *7*, 1564.
(36) Huang, X. Q.; Pelegri, A. A. *J. Eng. Mater. Technol., Trans. ASME* **2003**, *125*, 361.
(37) Lau, K. K. S.; Murthy, S. K.; Lewis, H. G. P.; Caulfield, J. A.; Gleason, K. K. *J. Fluorine Chem.* **2003**, *122*, 93.

(38) Hwang, N. M.; Cheong, W. S.; Yoon, K. D. *J. Cryst. Growth* **2000**, *218*, 33.
(39) Lin-Vien, D.; Colthup, N. B.; Fateley, W. G.; Grasselli, J. G. *The Handbook of Infrared and Raman Characteristic Frequencies of Organic Molecules*; Academic Press: San Diego, CA, 1991.
(40) Wenzel, R. N. *J. Phys. Colloid Chem.* **1949**, *53*, 1466.
(41) Thunemann, A. F.; Lieske, A.; Paulke, B. R. *Adv. Mater.* **1999**, *11*, 321.
(42) Zisman, W. A. *Ind. Eng. Chem.* **1963**, *55*, 18.
(43) Girifalco, L. A.; Good, R. J. *J. Phys. Chem.* **1957**, *61*, 904.
(44) Fowkes, F. M. *J. Phys. Chem.* **1962**, *66*, 382.
(45) Yasuda, T.; Okuno, T.; Yasuda, H. *Langmuir* **1994**, *10*, 2435.
(46) Hunt, M. O.; Belu, A. M.; Linton, R. W.; Desimone, J. M. *Macromolecules* **1993**, *26*, 4854.

MA052591P